Reactive and Functional Polymers 120 (2017) 14–19

Contents lists available at ScienceDirect

Reactive and Functional Polymers

journal homepage: www.elsevier.com/locate/react

Synthesis of polyfluorene and oligofluorene with N_1-hexylcytosine side chains and their sensing ability for nucleosides

Isao Yamaguchi*, Koji Miyawaki

Department of Chemistry, Interdisciplinary Graduate School of Faculty of Science and Engineering, Shimane University, 1060 Nishikawatsu, Matsue 690-8504, Japan

ARTICLE INFO

Keywords:
Polyfluorene
Oligofluorene
Nucleoside
Photoluminescence
Stern-Volmer constant

ABSTRACT

Polyfluorene (PF) and oligofluorene (OF) with N_1-hexylcytosine side chains were synthesized by Pd-complex-catalyzed condensation reactions starting from a newly synthesized monomer. The UV–vis spectra of the PF exhibit the absorption maximum at a longer wavelength than that of the OF, thus revealing that a π-conjugation system extends along the polymer chain. The PF and OF are photoluminescent in solution, and their photoluminescence (PL) intensities are gradually decreased by the addition of nucleosides such as adenosine, cytidine, and guanosine to the solution. The decrease in PL intensity is likely caused by photoinduced charge transfer (PCT) from the PF's and OF's backbones to the nucleosides, within the complexes generated by hydrogen bonding between the PF and OF cytosine group at their side chains and the nucleosides. Among the nucleosides, guanosine acted as the most effective PL quenching agent. Cyclic voltammetry (CV) analysis of the OF showed that it is electrochemically active.

1. Introduction

π-Conjugated polymers (CPs) are used for the trace detection of analytes, because their properties such as conductivity, emission intensity, and exciton migration are easily affected by external agents, leading to substantial changes in measurable signals [1–5]. These changes are based on electrostatic and non-covalent interactions between CPs and analytes.

Telomeres are essential parts of human chromosomes that regulate how our cells age. In humans, they consist of the same sequence of nucleotides, namely TTAGGG, and can reach up to 15,000 base pairs in length [6]. Telomerase is found at high levels in cancer cells. This enables cancer cells to continue replicating themselves indefinitely. To obtain information about telomerase activity, telomere chain lengths measurements are performed by several methods [7–17]. Unfortunately, these methods need several hours to be completed and often require polymerase chain reaction (PCR) amplification, which is also time consuming [7,8,9,12,14,16]. The introduction of nucleobases in luminescent CPs could be one of the best methods for the development of sensing materials for telomeres. The formation of hydrogen bonds between the CPs nucleobases and complementary nucleobases of telomeres should affect the CPs luminescent properties. Monitoring luminescence changes of CPs will enable short-time detection of nucleobases. In this study, luminescent PF and OF with nucleobase anchored groups were synthesized by Pd-complex-catalyzed condensation reactions. We introduced N_1-hexylcytosine side chains in the PF and OF because cytosine is complementary with guanine, which accounts for 50% of the nucleobases in telomeres. In addition to the N_1-hexylcytosine side chain, bromohexyl side chains were also introduced in the OF. The heavy Br atom can reduce motility of the alkyl side chain, which contributes to avoid photoluminescence (PL) decrease. In addition, the alkyl substituents' motility in luminescent aromatic oligomers sometimes leads to PL decrease [18]. Several papers concerning nucleobase sensors based on CPs have been reported [19–21]. These sensors were used for the detection of Cu(II) ions and nucleobase analogs such as 2,6-diacetamidopyrimidines. To the best of our knowledge, however, the synthesis of highly luminescent PF and OF with anchored nucleobases has not been reported to date. Besides, investigation of the chemical properties of such CPs could provide fundamental information for the development of new functional materials. Furthermore, CPs with N_1-alkylcytosine side groups may also be useful materials for sensing different proteins.

In this study, we report the synthesis of PF and OF with N_1-hexylcytosine side chains, their chemical properties, and sensing ability for detecting nucleosides such as adenosine, cytidine, and guanosine. A comparison between the OF's optical and electrochemical properties with those of the PF, as well as their nucleosides sensing ability is also made and offers valuable information.

* Corresponding author.
E-mail address: iyamaguchi@riko.shimane-u.ac.jp (I. Yamaguchi).

http://dx.doi.org/10.1016/j.reactfunctpolym.2017.09.001
Received 29 July 2017; Received in revised form 6 September 2017; Accepted 8 September 2017
Available online 09 September 2017
1381-5148/

2. Experimental

2.1. General

Solvents were dried, distilled, and stored under nitrogen. 2,7-Dibromo-9,9-bis(6′-bromohexyl)fluorene and poly(9,9-di-*n*-hexylfluorenyl-2,7-diyl) were synthesized according to the literature [1,2,22]. 9,9-Dihexylfluorene-2,7-trimethyleneborate (monomer-3) and the other reagents were purchased and used without further purification. Reactions were then performed with standard Schlenk techniques under nitrogen.

IR and NMR spectra were recorded on a JASCO FT/IR-660 PLUS spectrophotometer with a KBr pellet and JEOL AL-400 ECX-500 spectrometers, respectively. ESI TOF-MS analysis was conducted on a Bruker micrOTOFII. GPC analysis was then performed on a TOSO HLC-8220 with polystyrene gel columns (Shodex LF-804) with a RI detector using *N*,*N*-dimethylformamide (DMF) containing 0.06 M LiBr as an eluent. UV–vis and PL spectra were obtained using a JASCO V-560 spectrometer and a JASCO FP-6200, respectively. Cyclic voltammetry was performed with a Hokuto Denko HSV-110, and 1 cm × 1 cm and 1 cm × 2 cm Pt plates and Pt wire were used as working, counter, and reference electrodes, respectively. Tetraethylammonium tetrafluoroborate was used as an electrolyte. The scan speed was 50 mV s^{-1}.

2.2. Synthesis of monomer-1

NaH (0.29 g, 12 mmol) was dissolved in 30 mL of anhydrous dimethyl sulfoxide (DMSO) at 75 °C, and the solution was cooled to 30 °C. After cytosine (1.33 g, 12 mmol) was added to the solution, the reaction solution was stirred for 30 min, followed by the addition of 2,7-dibromo-9,9-bis(6′-bromohexyl)fluorene (1.95 g, 3.0 mmol). After stirring for 20 h at 30 °C, the solvent was removed under vacuum. The resulting solid was washed with chloroform (100 mL) and then with water (100 mL) at 60 °C. Monomer-1 was collected by filtration, dried under vacuum, and obtained as a white solid (0.73 g, 33%). ^{1}H NMR (400 MHz, DMSO-d_6): δ 7.80 (J = 10.4 Hz, 2H, 7.70 (s, 2H), 7.53 (dd, J = 1.6 and 8.0 Hz, 2H), 7.44 (d, J = 7.2 Hz, 2H), 6.93 (br, 4H), 5.58 (d, J = 6.8 Hz, 2H), 3.48 (t, J = 7.6 Hz, 4H), 2.00 (t, J = 7.6 Hz, 4H), 1.34 (s, 8H), 0.45 (s, 4H). ^{13}C NMR (125 MHz, DMSO-d_6): δ 165.32, 155.03, 151.91, 144.92, 138.22, 129.49, 125.56, 121.16, 120.23, 92.34, 54.91, 47.85, 28.09, 27.82, 24.90, 22.69. ESI TOF-MS Calcd. for $C_{33}H_{38}Br_2N_6O_2$: 711.1478. Found: 711.1482.

2.3. Synthesis of monomer-2

Pd(dppf)Cl_2 (0.10 g, 0.14 mmol) was added to dry 1,4-dioxane solution (20 mL) of 2-bromo-9,9′-bis(6′-bromohexyl)fluorene (1.15 g, 2.0 mmol), bis(pinacolato)diboron (0.61 g, 2.4 mmol), and potassium acetate (1.37 g, 14.0 mmol). After the reaction solution was stirred at 85 °C for 12 h, the solvent was removed under vacuum. The resulting solid was extracted with chloroform, dried over anhydrous sodium sulfate, and purified by silica gel column chromatography (eluent = $CHCl_3$). The solvent was removed by evaporation and dried under vacuum to give monomer-2 as a light yellow paste (0.92 g, 74%). ^{1}H NMR (400 MHz, $CDCl_3$): δ 7.81 (d, J = 7.6 Hz, 1H), 7.69–7.73 (m, 3H), 7.29–7.34 (m, 3H), 3.26 (t, J = 6.8 Hz, 4H), 1.99 (m, 4H), 1.63 (m, 4H), 1.19 (m, 4H), 1.06 (m, 4H), 0.59 (m, 4H). ^{13}C NMR (125 MHz, DMSO-d_6): δ 150.81, 149.38, 144.02, 140.82, 133.77, 128.63, 127.53, 126.75, 122.75, 120.10, 118.96, 83.67, 54.89, 40.00, 33.86, 32.58, 28.94, 27.69, 24.93, 23.39. ESI TOF-MS Calcd. for $C_{31}H_{43}BBr_2O_2$: 619.1783. Found: 619.1788.

2.4. Synthesis of polymer-1

$Pd(PPh_3)_4$ (0.011 g, 0.0097 mmol) was dissolved in 8 mL of dry DMSO under N_2. Monomer-1 (0.071 g, 0.10 mmol) and monomer-3 (0.050 g, 0.10 mmol) were then added to the solution. After K_2CO_3(aq) (2.5 M, 8 mL; N_2 bubbled before use) was added dropwise to the solution, the mixture was stirred at 105 °C for 48 h. The precipitate was collected by filtration, washed with water, and dried under vacuum to give polymer-1 as a very thin green powder (0.080 g, 86%). ^{1}H NMR (400 MHz, DMSO-d_6): δ 7.55–7.93 (12H), 7.33 (2H), 6.54 (4H), 5.59 (2H), 3.50 (4H), 2.07–2.16 (8H), 1.40 (6H), 1.08 (24H), 0.79 (2H), 0.73 (6H).

2.5. Synthesis of oligomer-1

$Pd(PPh_3)_4$ (0.028 g, 0.024 mmol) was dissolved in 3 mL of dry DMSO under N_2. Monomer-1 (0.11 g, 1.5 mmol) and monomer-2 (0.19 g, 3.0 mmol) were added to the solution. After K_2CO_3(aq) (2.5 M, 3 mL; N_2 bubbled before use) was added dropwise to the solution, the mixture was stirred at 90 °C for 48 h. The precipitate was then filtered, and the solvent of the filtrate was removed under vacuum. The resulting solid was extracted with methanol, and the solvent was removed under vacuum to give oligomer-1 as a light brown powder (0.039 g, 17%). ^{1}H NMR (400 MHz, DMSO-d_6): δ 7.31–7.83 (22H), 6.92 (4H), 5.56 (2H), 4.20 (4H), 3.47 (4H), 3.22 (4H), 1.98 (12H), 1.33 (4H), 1.17 (4H), 1.00 (28H), 0.46 (12H).

3. Results and discussion

3.1. Synthesis

To obtain the polymers and the oligomer with N_1-hexylcytosine side chains, a new monomer, namely monomer-1, was synthesized by the reactions shown in Scheme 1. The structure of monomer-1 was determined by ^{1}H and ^{13}C NMR, and ESI TOF-MS spectroscopy. The polymer with N_1-hexylcytosine side chains, namely polymer-1, was

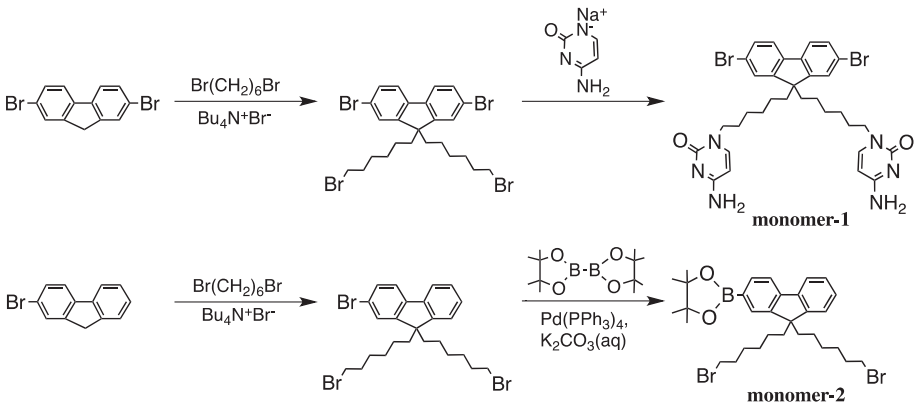

Scheme 1. Synthesis of monomers.

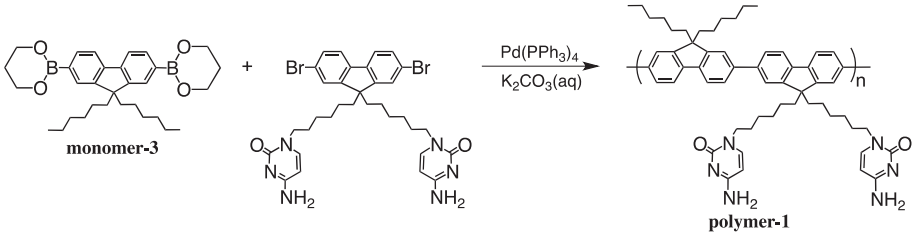

Scheme 2. Synthesis of polymer.

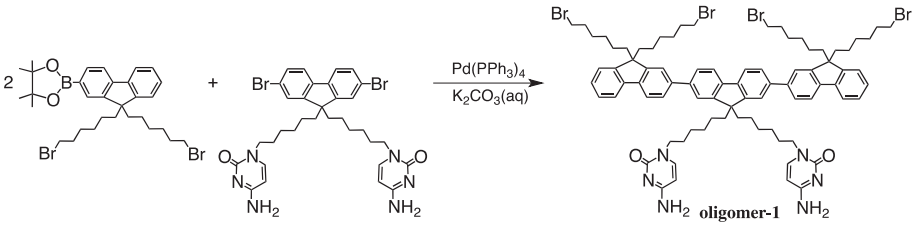

Scheme 3. Synthesis of oligomer.

synthesized by the Pd-complex-catalyzed polycondensation of monomer-1 with monomer-3 (Scheme 2). To obtain information about the polymers' structure and their structure-properties relationship, oligomer-1 was synthesized by the reaction of monomer-2 with monomer-1 in a 2:1 M ratio (Scheme 3).

Monomer-1 is soluble in acetone, chloroform, DMSO, and methanol at room temperature. Monomer-2 and oligomer-1 are soluble in DMF and DMSO at 100 °C. Polymer-1 is partly soluble in the solvents at 100 °C, but it is insoluble at room temperature. Although the solubility of polymer-1 is somewhat low, the UV–vis and PL measurements of the polymer can be performed. The low solubility of PF and OF with the N_1-hexylcytosine side chains is ascribed to the formation of intra- and intermolecular hydrogen bonds involving cytosine groups. Especially in polymer-1, the intermolecular hydrogen bonds may lead to complicated conformations such as cross-linking structures in solution.

The GPC measurements suggest that the M_n and M_w values of the DMF soluble part of polymer-1 are 7180 and 7670, respectively.

3.2. IR and ^{1}H NMR spectra

Fig. 1 shows the IR spectra of monomer-1, monomer-3, polymer-1, and oligomer-1. The IR spectrum of monomer-3 contained peaks corresponding to the stretching vibrations of C—H bonds of the methylene groups at 2977 cm^{-1} and those of B—O bonds at 1349 cm^{-1}, respectively. The peaks corresponding to the later bonds are not present in the IR spectra of polymer-1 and oligomer-1. These observations suggest that the expected condensation reactions were performed successfully. The peaks corresponding to the N—H bonds and C═O bonds stretching vibrations of polymer-1 and oligomer-1 are observed at 3345 cm^{-1} and 1650 cm^{-1} and 3348 cm^{-1} and 1654 cm^{-1}, respectively. These wavenumbers are essentially the same as those of monomer-1 (ν_{N-H} = 3349 cm^{-1} and $\nu_{C=O}$ = 1649 cm^{-1}).

Fig. 2 shows the ^{1}H NMR spectra of monomer-1, oligomer-1, and polymer-1, which were almost dissolved in DMSO-d_6 at 100 °C. The peak assignments are shown in the figure. The peak integral ratios of the aromatic and aliphatic protons of polymer-1 and oligomer-1 suggested that the expected condensation reactions were performed successfully. The peaks corresponding to the cytosine protons (H^e and H^d) of monomer-1 appear at δ 5.58 and 7.44, respectively. The corresponding peaks of polymer-1 and oligomer-1 appear essentially in the same positions as those of monomer-1. The peaks corresponding to the NH_2 groups of monomer-1 and oligomer-1 appear at lower magnetic field positions than those of polymer-1. These observations correspond to the assumption that the cytosine group of monomer-1 and oligomer-1 can form intermolecular hydrogen bonds more easily than that of the polymers.

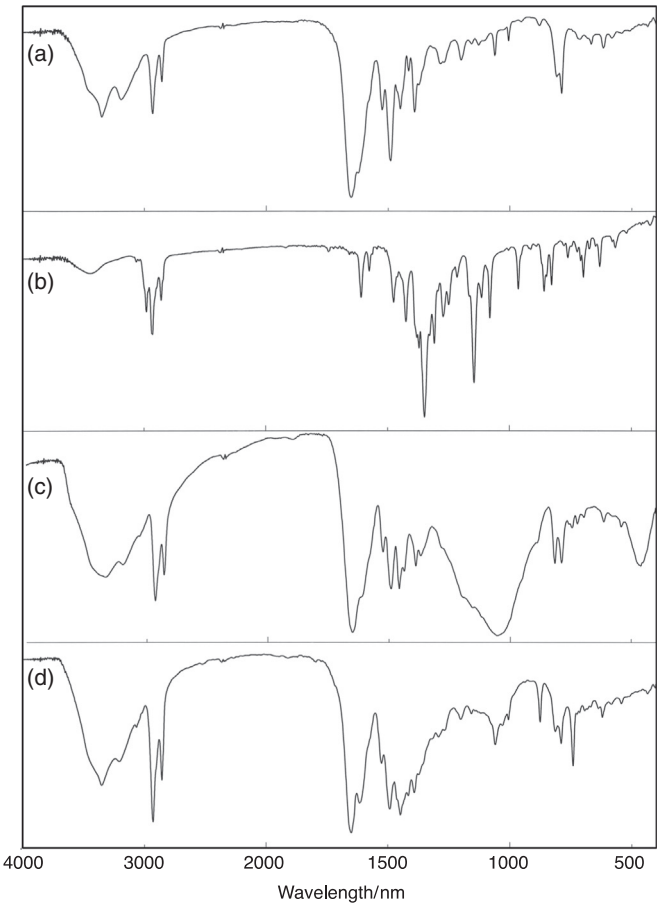

Fig. 1. IR spectra of (a) monomer-1, (b) monomer-3, (c) polymer-1, and (d) oligomer-1.

3.3. Cyclic voltammograms

Fig. 3 shows the cyclic voltammogram of a cast film of oligomer-1 in an acetonitrile solution containing tetramethylammonium tetrafluoroborate at 0.10 M concentration. The cast film of oligomer-1 exhibited peaks at 0.75 V (E_{pa} vs. Ag^+/Ag) and − 1.51 V (E_{pc} vs. Ag^+/Ag) corresponding to the electrochemical oxidation of the oligomer backbone and reduction of the cytosine group, respectively. The CV

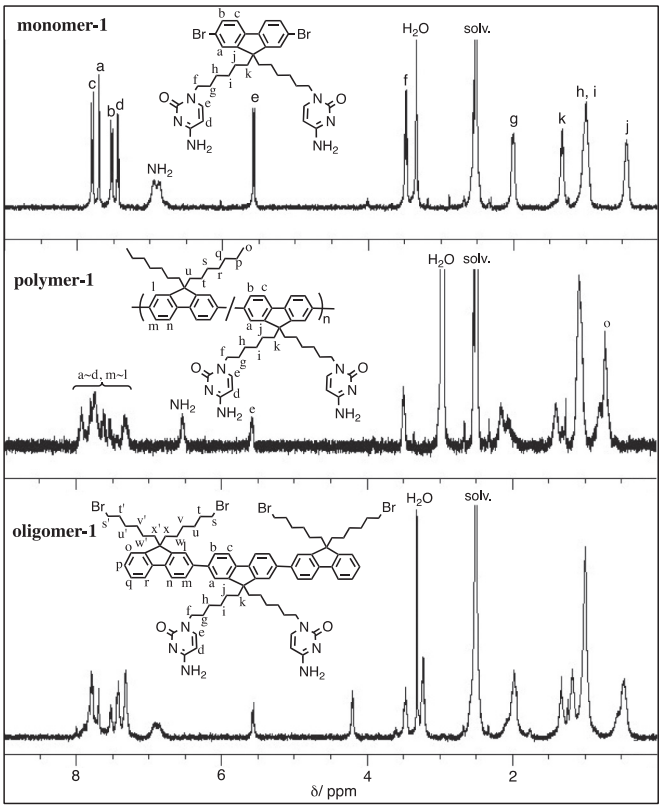

Fig. 2. ^{1}H NMR spectra of the DMSO-d_6 solution of monomer-1 and DMSO-d_6 soluble part of polymer-1 and oligomer-1.

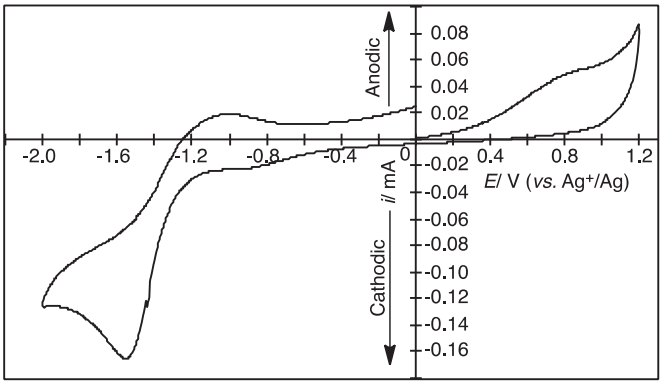

Fig. 3. Cyclic voltammogram of the cast film of oligomer-1 on a Pt plate in an acetonitrile solution containing $[Et_4N]BF_4$ (0.10 M).

measurement of polymer-1 was not possible due to its low solubility. The highest occupied molecular orbital (HOMO) energy level of oligomer-1 was estimated by approximately − 5.2 eV, according to the following Equation [23],

$$\text{HOMO} = -(4.71 + E_{\text{onset}})$$

where E_{onset} is the onset potential value of the oxidation peak. The lowest unoccupied molecular orbital (LUMO) energy level of oligomer-1 was calculated by − 2.0 eV from the HOMO energy level and the optical band gap of oligomer-1 (E_g = 3.2 eV) that was estimated from the onset position (λonset).

3.4. UV–vis and photoluminescence spectra

Fig. 4 shows the UV–vis spectra of monomer-1, polymer-1, and oligomer-1 in DMSO. The absorption corresponding to the cytosine

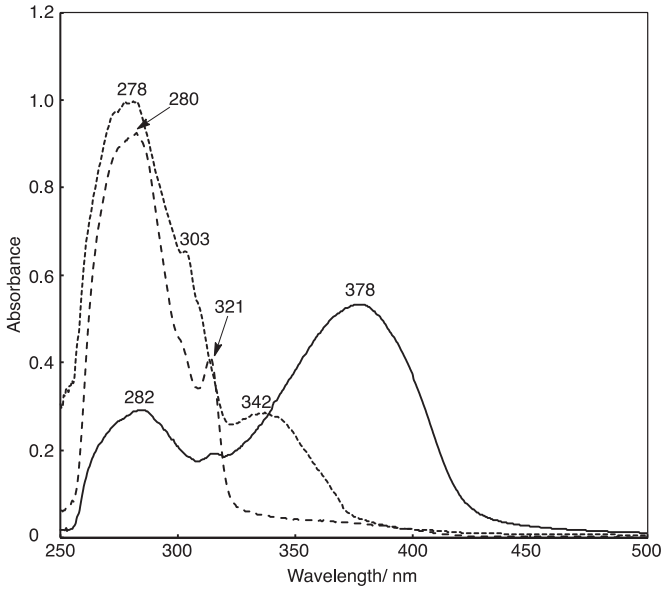

Fig. 4. UV–vis spectra of monomer-1 (hashed curve), polymer-1 (solid curve), and oligomer-1 (dotted curve) in DMSO.

groups of monomer-1, polymer-1, and oligomer-1 appears at around 280 nm. The λonset of the absorption spectrum of oligomer-1 appears at a longer wavelength than that of monomer-1; this suggests that a larger π-conjugation system is present in oligomer-1. The absorption maximum (λmax) and λonset of the absorption spectrum of polymer-1 appear at a longer wavelength than those of oligomer-1. These observations are attributed to the more expanded π-conjugation system of the polymer.

The polymer and oligomer obtained in this study are photoluminescent in solutions when irradiated with UV light. The PL peak position of polymer-1 (λem = 421 nm) appears at a longer wavelength than that of oligomer-1 (λem = 324 nm), which is attributed to the larger π-conjugated system present in the polymer chain. These observations are consistent with the results that the absorptions of the polymer are observed at longer wavelengths than that of the oligomer.

The PL intensity of the DMSO solutions of polymer-1 and oligomer-1 decreased upon addition of adenosine, cytidine, and guanosine to the solutions. This suggests that these nucleosides worked as quenchers of the polymers and oligomer PL. Recent studies of binary conjugated polymer blends highlight the competition between energy transfer and photoinduced charge transfer (PCT) events as a function of the HOMO and LUMO energy levels in the donor and acceptor pairs [24–26]. When both the HOMO and LUMO energy levels are higher in one of the optical partners, donor excitation would lead to PCT to the acceptor [1,2,27–30]. As described, the HOMO and LUMO energy levels of oligomer-1 were − 5.2 eV and − 2.0 eV, respectively. These levels are higher than those of the nucleosides used in this study, as summarized in Table 1 [31]. Fig. 5 shows a possible quenching mechanism of polymer and oligomer PL in the presence of these nucleosides. When the cytosine groups of the polymer and oligomer (donors) form complexes with the nucleosides (acceptors), donor excitation causes PCT to

Table 1
HOMO and LUMO energy levels (unit; eV) of oligomer-1 and nucleosides.

	Oligomer-1	Guanosine	Adenosine	Thymidine
LUMO	− 2.0[a]	− 2.20[c]	− 2.25[c]	− 2.70[c]
HOMO	− 5.2[b]	− 6.25[c]	− 6.50[c]	− 6.80[c]

[a] Calculated by the difference between the optical band gap and HOMO energy level.
[b] Determined by cyclic voltammetry.
[c] Data from reference 31.

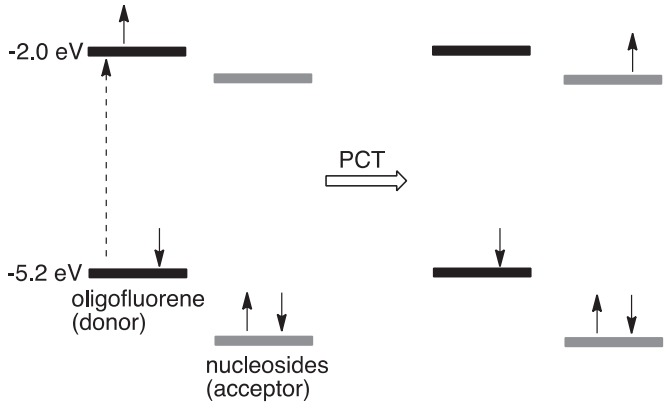

Fig. 5. A possible quenching mechanism for the PL of the oligomer in the presence of the nucleosides.

the acceptor's LUMO. In this situation, the polymer and oligomer PL are quenched. This assumption is confirmed by the fact that the poly(9,9-di-*n*-hexylfluorenyl-2,7-diyl)'s PL intensity is almost unchanged by the addition of these nucleosides.

Fig. 6 shows the PL spectra of polymer-1 and oligomer-1 in the presence of a series of concentrations of guanosine, which acts as PL quencher. PL intensities decreased with an increase in guanosine concentration. A quantitative measurement of PL quenching can be achieved by determining the Stern-Volmer constant, K_{SV}, from the following equation:

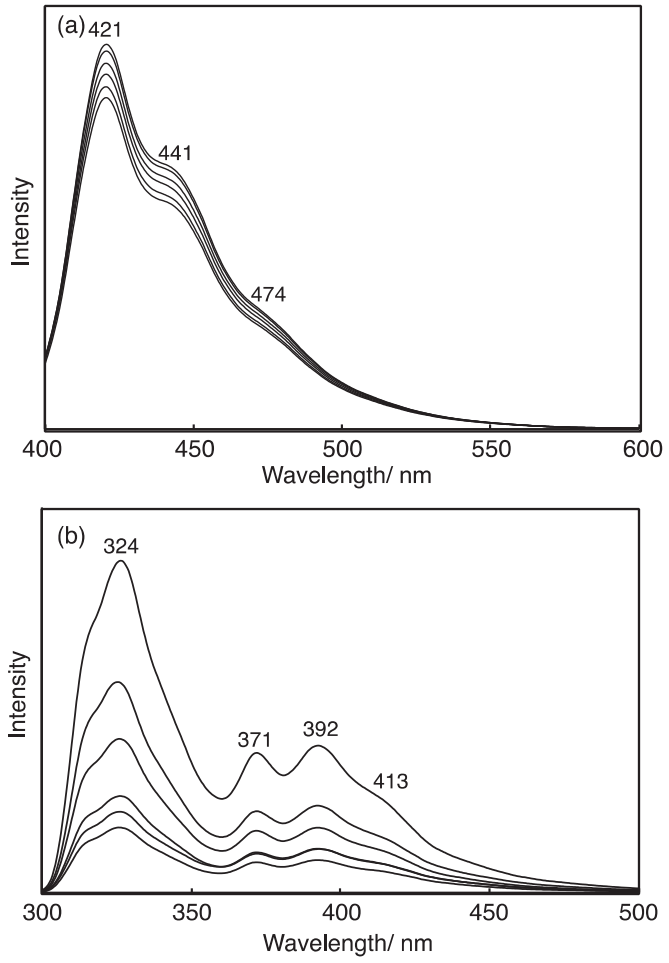

Fig. 6. PL spectra of (a) polymer-1 and (b) oligomer-1 in the presence of a series of concentrations of guanosine.

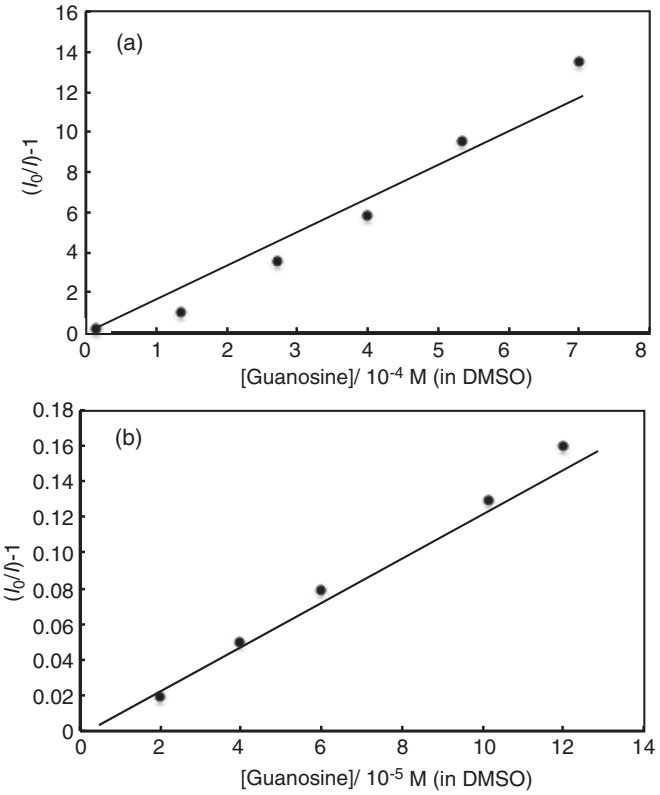

Fig. 7. Stern-Volmer plots for PL quenching by guanosine for (a) polymer-1 and (b) oligomer-1.

$$I_0/I = 1 + K_{SV}[\text{quencher}]$$

where I_0 is the PL intensity in the absence of quencher and I is the PL intensity in the presence of quencher. This equation reveals that I_0/I increases in direct proportion to the quenching moiety's concentration, and the constant K_{SV} defines the efficiency of quenching. Fig. 7 shows Stern-Volmer plots for PL quenching by guanosine for polymer-1 and oligomer-1. The K_{SV}(G) values of polymer-1 and oligomer-1 are $5.5 \times 10^3\ M^{-1}$ and $2.0 \times 10^4\ M^{-1}$, respectively. The higher K_{SV}(G) value of oligomer-1 than that of polymer-1 can be attributed to the easier formation of an associate complex between the oligomer and guanosine. This is based on the assumption that polymer-1 takes more complicated conformations than oligomer-1 in solution. The K_{SV}(A) and K_{SV}(C) values of oligomer-1 for PL quenching by adenosine and thymidine are $1.2 \times 10^4\ M^{-1}$ and $1.0 \times 10^4\ M^{-1}$, respectively. The differences (Δ_{LUMO}) of the LUMO levels between oligomer-1 and guanosine, adenosine, and thymidine are 0.20 eV, 0.25 eV, and 0.70 eV, respectively. The fact that the K_{SV} values of oligomer-1 increase with the decrease of the Δ_{LUMO} values corresponds to the assumption that PL quenching by the nucleotides is attributed to PCT from the LUMO level of the oligomer to those of the nucleotides. The hydrogen bonds between oligomer-1 and nucleotides also contribute to PL quenching. The higher K_{SV}(G) value than the K_{SV}(A) and K_{SV}(C) values corresponds to the formation of strong hydrogen bonds between oligomer-1 and guanosine. Cytosine can form hydrogen bonds with guanosine at three positions and with adenosine and thymidine at less than two positions.

4. Conclusions

Polyfluorene (PF) and oligofluorene (OF) with N_1-hexylcytosine side chains were synthesized by Pd-complex-catalyzed condensation reactions. The UV–vis spectra of the PF exhibit absorption maxima at longer wavelengths than in the case of the OF, revealing that the π-conjugation system expands along the polymer chains. The PF and OF are

photoluminescent in solution, and their photoluminescence (PL) intensities are decreased by the addition of nucleosides such as adenosine, thymidine, and guanosine to the solution. It is hypothesized that the decrease in PL intensity is caused by photoinduced charge transfer (PCT) in the complex generated by hydrogen bonding between the PF and OF cytosine group and the nucleosides. Among the nucleosides tested, guanosine showed the most effective PL quenching activity. The results correspond to the following: (i) the cytosine groups of the PF and OF form more stable complexes with guanosine than adenosine and thymidine, and (ii) PCT occurs easily in the complex of oligomer-1 with guanosine because of the smaller Δ_{LUMO} between oligomer-1 and guanosine than those between oligomer-1 and the other nucleotides. The solubility of the PF and OF obtained in this study was low, but the detection of nucleotides was possible by PL measurements of the soluble parts of the PF and OF. Introduction of hydrophilic groups in PF and OF will be conducted to improve their solubility in future studies. Cyclic voltammetry analysis suggests that the OF undergoes electrochemical oxidation of the backbone and electrochemical reduction of the cytosine group. From the results obtained in this study, PF and OF could be useful materials for determining telomere chain lengths within shorter times than the currently used methods.

References

[1] B. Liu, B.S. Gaylord, S. Wang, G.C. Bazan, Effect of chromophore-charge distance on the energy transfer properties of water-soluble conjugated oligomers, J. Am. Chem. Soc. 125 (2003) 6705–6714.

[2] B. Liu, G.C. Bazan, Optimization of the molecular orbital energies of conjugated polymers for optical amplification of fluorescent sensors, J. Am. Chem. Soc. 128 (2006) 1188–1196.

[3] D. Zeng, J. Cheng, S. Ren, J. Sun, H. Zhong, E. Xu, J. Du, Q. Fang, A new sensor for copper(II) ion based on carboxyl acid groups substituted polyfluoreneethynylene, React. Funct. Polym. 68 (2008) 1715–1721.

[4] H.F. Leng, W.H. Wu, Synthesis of a novel fluorene-based conjugated polymer with pendent bulky caged adamantane moieties and its application in the detection of trace DNT explosives, React. Funct. Polym. 72 (2012) 206–211.

[5] H. Fukumoto, Y. Kase, T. Koizumi, T. Yamamoto, Preparation and chemical properties of π-conjugated poly(1,10-phenanthroline-3,8-diyl)s with crown ether subunits, React. Funct. Polym. 82 (2014) 9–16.

[6] V.A. Zakian, Telomers: beginning to understand the end, Science 270 (1995) 1601–1607.

[7] R.C. Allshire, J.R. Gosden, S.H. Cross, G. Cranston, D. Rout, N. Sugawara, J.W. Szostak, P.A. Fantes, N.D. Hastie, Telomeric repeat from *T. thermophila* cross hybridizes with human telomeres, Nature 332 (1988) 656–659.

[8] C.B. Harley, A.B. Futcher, C.W. Greider, Telomeres shorten during ageing of human fibroblasts, Nature 345 (1990) 458–460.

[9] P.M. Lansdorp, N.P. Verwoerd, F.M. van de Rijke, V. Dragowska, M.T. Little, R.W. Dirks, A.K. Raap, H.J. Tanke, Heterogeneity in telomere length of human chromosomes, Hum. Mol. Genet. 5 (1996) 685–691.

[10] S.S. Poon, U.M. Martens, R.K. Ward, P.M. Lansdorp, Telomere length measurements using digital fluorescence microscopy, Cytometry 36 (1999) 267–278.

[11] G.M. Baerlocher, J. Mak, T. Tien, P.M. Lansdorp, Telomere length measurement by fluorescence in situ hybridization and flow cytometry: tips and pitfalls, Cytometry 47 (2002) 89–99.

[12] R.M. Cawthon, Telomere measurement by quantitative PCR, Nucleic Acids Res. 30 (2002) e47.

[13] B. Brando, A. Longo, B. Beltrami, D. Passoni, R. Verna, F. Licastro, M.M. Corsi, Determination of telomere length by flow-fluorescence in situ hybridization in Down's syndrome patients, Int. J. Tissue React. 26 (2004) 61–64.

[14] R.M. Cawthon, Telomere length measurement by a novel monochrome multiplex quantitative PCR method, Nucleic Acids Res. 37 (2009) e21.

[15] M. Kimura, R.C. Stone, S.C. Hunt, J. Skurnick, X. Lu, X. Cao, C.B. Harley, A. Aviv, Measurement of telomere length by the southern blot analysis of terminal restriction fragment lengths, Nat. Protoc. 5 (2010) 1596–1607.

[16] T. Ishizuka, Y. Xu, M. Komiyama, A chemistry-based method to detect individual telomere length at a single chromosome terminus, J. Am. Chem. Soc. 135 (2013) 14–17.

[17] A. Sasaki, S. Ide, Y. Kawamoto, T. Bando, Y. Murata, M. Shimura, K. Yamada, A. Hirata, K. Nokihara, T. Hirata, H. Sugiyama, K. Maeshima, Telomere visualization in tissue sections using pyrrole–imidazole polyamide probes, Sci Rep 6 (2016) 29261.

[18] G. Martinelli, G.M. Farinola, V. Pinto, A. Cardone, Synthetic aspects and electro-optical properties of fluorinated arylenevinylenes for luminescence and photovoltaics, Materials 6 (2013) 1205–1236.

[19] P.K. Lo, H.F. Sleiman, Synthesis and molecular recognition of conjugated polymer with DNA-mimetic properties, Macromolecules 41 (2008) 5590–5603.

[20] P.K. Lo, H.F. Sleiman, Nucleobase-templated polymerization: copying the chain length and polydispersity of living polymers into conjugated polymers, J. Am. Chem. Soc. 131 (2009) 4182–4183.

[21] C. Xing, H. Yuan, S. Xu, H. An, R. Niu, Y. Zhan, Nucleobase-functionalized conjugated polymer for detection of copper(II), ACS Appl. Mater. Interfaces 6 (2014) 9601–9607.

[22] I.O. Huyal, U. Koldemir, T. Ozel, H.V. Demir, D. Tuncel, On the origin of high quality white light emission from a hybrid organic/inorganic light emitting diode using azide functionalized polyfluorene, J. Mater. Chem. 18 (2008) 3568–3574.

[23] G. Zhang, Y. Fu, Z. Xie, Q. Zhang, Low bandgap polymers with benzo [1,2-b:4,5-b′] dithiophene and bisthiophene-dioxopyrrolothiophene units for photovoltaic applications, Polymer 52 (2011) 415–421.

[24] J.J.M. Halls, J. Cornil, D.A. Santos, R. Silbey, D.H. Hwang, A.B. Holmes, J.L. Brédas, R.H. Friend, Resonant multiple Andreev reflections in mesoscopic superconducting junctions, Phys. Rev. B 60 (1999) 5721.

[25] J.L. Segura, R. Gómez, N. Martún, C. Luo, A. Swartz, D.M. Guldi, Variation of the energy gap in fullerene-based dendrons: competitive *versus* sequential energy and electron transfer events, Chem. Commun. (8) (2001) 707–708.

[26] D.M. Guldi, A. Swartz, C. Luo, R. Gómez, J. Segura, N. Martún, Rigid dendritic donor – acceptor ensembles: control over energy and electron transduction, J. Am. Chem. Soc. 124 (2002) 10875–10886.

[27] N.S. Sariciftci, L. Smilowitz, A.J. Heeger, F. Wudl, Photoinduced electron transfer from a conducting polymer to buckminsterfullerene, Science 258 (1992) 1474–1476.

[28] Q.H. Xu, D. Moses, A.J. Heeger, Time-resolved measurements of photoinduced electron transfer from polyfluorene to C60, Phys. Rev. B 67 (2003) 245417.

[29] J.L. Brédas, D. Beljonne, V. Coropceanu, J. Cornil, Charge-transfer and energy-transfer processes in π-conjugated oligomers and polymers: a molecular picture, Chem. Rev. 104 (2004) 4971–5004.

[30] K.R.J. Thomas, A.L. Thompson, A.V. Sivakumar, A.J. Bardeen, S. Thayumanavan, Energy and electron transfer in bifunctional non-conjugated dendrimers, J. Am. Chem. Soc. 127 (2005) 373–383.

[31] Y. Youn, K. Jung, Y. Lee, S. Park, H. Lee, Y. Yi, Electronic structures of nucleosides as promising functional materials for electronic devices, J. Phys. Chem. C 121 (2017) 12750–12756.